

1 Stability of Pharmaceutical Cocrystal During
2 Milling: A Case Study of 1:1 Caffeine-Glutaric Acid

3 *Pui Shan Chow,^{*†}, Grace Lau,[†], Wai Kiong Ng,[†] and Venu R. Vangala^{†,‡}*

4 ¶

5 †Crystallisation and Particle Science

6 Institute of Chemical and Engineering Sciences

7 A*STAR (Agency for Science, Technology and Research)

8 1, Pesek Road, Jurong Island, Singapore, 627833.

9

10 ‡Current Affiliation:

11 Centre for Pharmaceutical Engineering Science

12 School of Pharmacy, University of Bradford

13 Bradford BD7 1DP, United Kingdom

14

15

16 **ABSTRACT:** Despite the rising interest in pharmaceutical cocrystals in the past decade, there is
17 a lack of research in the solid processing of cocrystals downstream to crystallization.
18 Mechanical stress induced by unit operations such as milling could affect the integrity of the

19 material. The purpose of this study is to investigate the effect of milling on pharmaceutical
20 cocrystal and compare the performance of ball mill and jet mill, using caffeine-glutaric acid (1:1)
21 cocrystal as the model compound. Our results show that ball milling induced polymorphic
22 transformation from the stable Form II to the metastable Form I; whereas Form II remained
23 intact after jet milling. Jet milling was found to be effective in reducing particle size but ball
24 milling was unable to reduce the particle beyond certain limit even with increasing milling
25 intensity. Heating effect during ball milling was proposed as a possible explanation for the
26 difference in the performance of the two types of mill. The local increase in temperature beyond
27 the polymorphic transformation temperature may lead to the conversion from stable to
28 metastable form. At longer ball milling duration, the local temperature could exceed the melting
29 point of Form I, leading to surface melting and subsequent recrystallization of Form I from the
30 melt and agglomeration of the crystals. The findings in this study have broader implications on
31 the selection of mill and interpretation of milling results for not only pharmaceutical cocrystals
32 but pharmaceutical compounds in general.

33 **Keywords:** Mechanical stress; Planetary ball milling; Jet milling; Polymorphic transformation;
34 Pharmaceutical cocrystal

35

36 ■ INTRODUCTION

37 Pharmaceutical cocrystal has been considered as a new class of drug compound with
38 great potential. This is primarily because the physicochemical properties of an active
39 pharmaceutical ingredient (API), such as solubility, dissolution rate, stability and hygroscopicity,

40 can be altered by forming cocrystal with a suitable coformer.¹⁻¹¹ As each cocrystal is considered
41 as a new molecular entity, cocrystal also offers new avenues for generating patents and
42 intellectual property that could create huge economic benefit.¹² It was once thought that
43 cocrystals have a lesser tendency to form polymorphs.¹³ However, the number of solid forms
44 known for a given compound is proportional to the time and money spent in research on that
45 compound.^{14, 15} With the rising interest in cocrystals in the past decade, polymorphs of many
46 cocrystals have been reported according to a database analysis in 2014.¹⁶ Cocrystals are just as
47 likely to exhibit polymorphism as single component crystals.¹⁷

48 With pharmaceutical cocrystal gaining prominence, research in cocrystal has been
49 actively pursued by many research groups. Most of the literature reports focus on the discovery
50 of novel cocrystals and their enhancement in physicochemical properties. Recently, there has
51 been major progress in the development of cocrystallisation processes that are amenable to
52 industrial production.¹⁸⁻²² However, research in the solid processing unit operations downstream
53 to crystallization is lacking. Solid processing such as milling, granulation and tableting all
54 induce mechanical stress and involve solvent exposure that could lead to solid form changes
55 (polymorph, solvate).^{23, 24} Dissociation into the constituent components could be an additional
56 concern for pharmaceutical cocrystal. Milling has been known to induce form changes to API
57 due to the high mechanical energy introduced.²⁵⁻³² Boldyreva has provided a comprehensive
58 review on the various views and concepts regarding mechanochemistry of inorganic and organic
59 systems.³³ De Gusseme et al.²⁶ has shown that the outcome of milling depends on the
60 temperature at which the milling was performed: amorphization occurred at temperature below
61 glass transition temperature (T_g) while polymorphic transformation took place at temperature
62 above T_g . In this work, we aim to study the effect of milling on the stability of pharmaceutical

63 cocrystal. The performance of two types of mill typically used in the industry, ball mill and jet
64 mill, is also compared.

65 Caffeine-glutaric acid (1:1) cocrystal (CA-GA) is chosen as the model compound in this
66 study. Caffeine (1,3,7-trimethyl-2,6-purinedione) is known to exhibit instability toward
67 moisture, with the formation of non-stoichiometric hydrate.³⁴ Trask et al. demonstrated that
68 CA-GA could be a remedy for caffeine hydration problem.⁹ Two polymorphs have been
69 identified for CA-GA (Forms I and II)^{9, 35} and their relative thermodynamic stability has recently
70 been thoroughly investigated.³⁶ Form I is needle-shaped or rod-shaped while Form II appears as
71 blocks.^{9, 36}

72 ■ EXPERIMENTAL SECTION

73 **Materials.** Anhydrous caffeine (99% purity) was obtained from Fluka and glutaric acid (99%)
74 from Alfa Aesar were used as received. The solvents were of analytical or chromatographic
75 grade. Form II of caffeine-glutaric acid cocrystal was obtained by seeded cooling solution
76 cocrystallization following the procedure described in Yu et al.²² Only sieved fraction between
77 355 and 600 μm was used in the milling experiments. The sieved crystals were divided into
78 equal portions using a rotary sample divider to ensure that the particle size distribution (PSD) of
79 the crystals used in each milling experiment was as similar as possible. Each portion was placed
80 in a small covered glass vial and stored at < 30% RH and room temperature prior to use. Particle
81 size distribution, particle morphology and polymorph of the milled samples were analyzed on the
82 same day as the milling experiments. This was to ensure that any changes incurred by the
83 milling process could be captured.

84 **Planetary Ball Milling.** Ball milling was performed using a Fritsch Pulverisette 5 (FRITSCH
85 GmbH, Idar-Oberstein, Germany), a planetary ball mill equipped with stainless steel jar and balls
86 (10 mm diameter). The mass ratio of ball to sample was kept at 20:1 and the rotation speed was
87 set at 100 rpm for all the runs. 2 g of sample was used in each ball milling run.

88 **Jet Milling.** Jet milling was performed using an Alpine spiral jet mill 50 AS (Hosokawa Alpine,
89 Germany). Samples were fed at 1 g/s and the injection and grinding pressures were varied to
90 investigate the effect of milling conditions. 5 g of sample was used in each jet milling run.

91 **Powder X-ray Diffraction (PXRD).** The powder diffraction data were collected in Bragg-
92 Brentano geometry with a Bruker D8 Advance (Bruker AXS GmbH, Germany) X-ray powder
93 diffractometer equipped with a Cu-K α radiation ($\lambda = 1.54056 \text{ \AA}$) source, a Nickel-filter, 0.3°
94 divergence slit and a linear position sensitive detector (Vantec-1). The diffractometer was
95 operated at 35 kV and 40 mA. The sample was loaded onto a glass circular sample holder of 1
96 mm thickness and 1.5 cm diameter. The data were collected over an angle range of 5 to $50^\circ 2\theta$ at
97 a scanning speed of $2^\circ 2\theta$ per minute.

98 **Particle Size Analysis.** The particle size distribution was measured using laser diffraction
99 (Malvern Mastersizer MS-2000, UK) with n-decane as the wet dispersion medium and at a pump
100 rate of 2000 rpm. Measurements were done in triplicate.

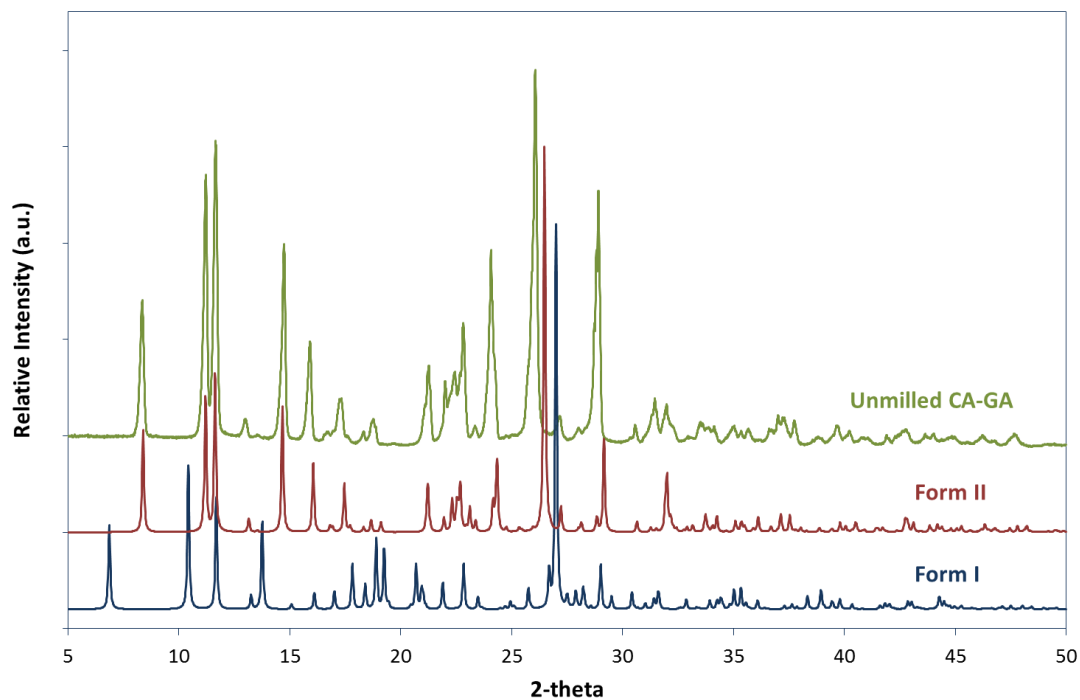
101 **Scanning Electron Microscopy.** The particle morphology was examined by high resolution
102 scanning electron microscopy (SEM, JSM-6700F, JEOL, Japan) operating at 5 kV. The samples
103 were coated with platinum for 1 min by a sputter coater (Cressington Sputter Coater 208HR,
104 UK) prior to analysis.

105 ▪ **RESULTS AND DISCUSSION**

106 **Characterization of Unmilled Cocryystals**

107 Before the milling experiments, the CA-GA cocryystals obtained by seeded cooling
108 crystallization²² were analyzed by PXRD to confirm that they belonged to Form II. As shown in
109 Figure 1, the PXRD pattern of the unmilled crystals corresponded to that of Form II. DSC was
110 also performed to confirm that the unmilled crystals corresponded to Form II (Figure S1,
111 Supplementary information, SI).

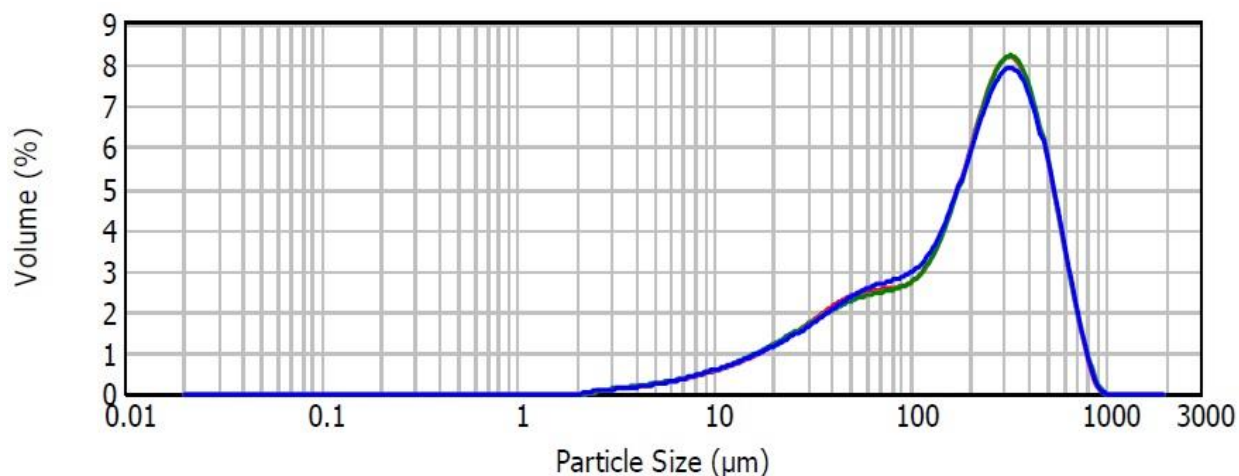
112



113

114 **Figure 1.** Powder X-ray diffraction pattern of unmilled caffeine-glutaric acid cocryystals
115 confirmed that the raw crystals belonged to Form II.

116 Since only 1-5 g of crystals were used in each milling experiment, it was difficult to obtain
117 reliable PSD by mechanical sieving. Therefore, PSDs measured by Malvern Mastersizer were
118 used as basis of comparison in this work. The PSD of the unmilled crystal is shown in Figure 2.
119 d_{50} of the raw crystal was 217 μm .



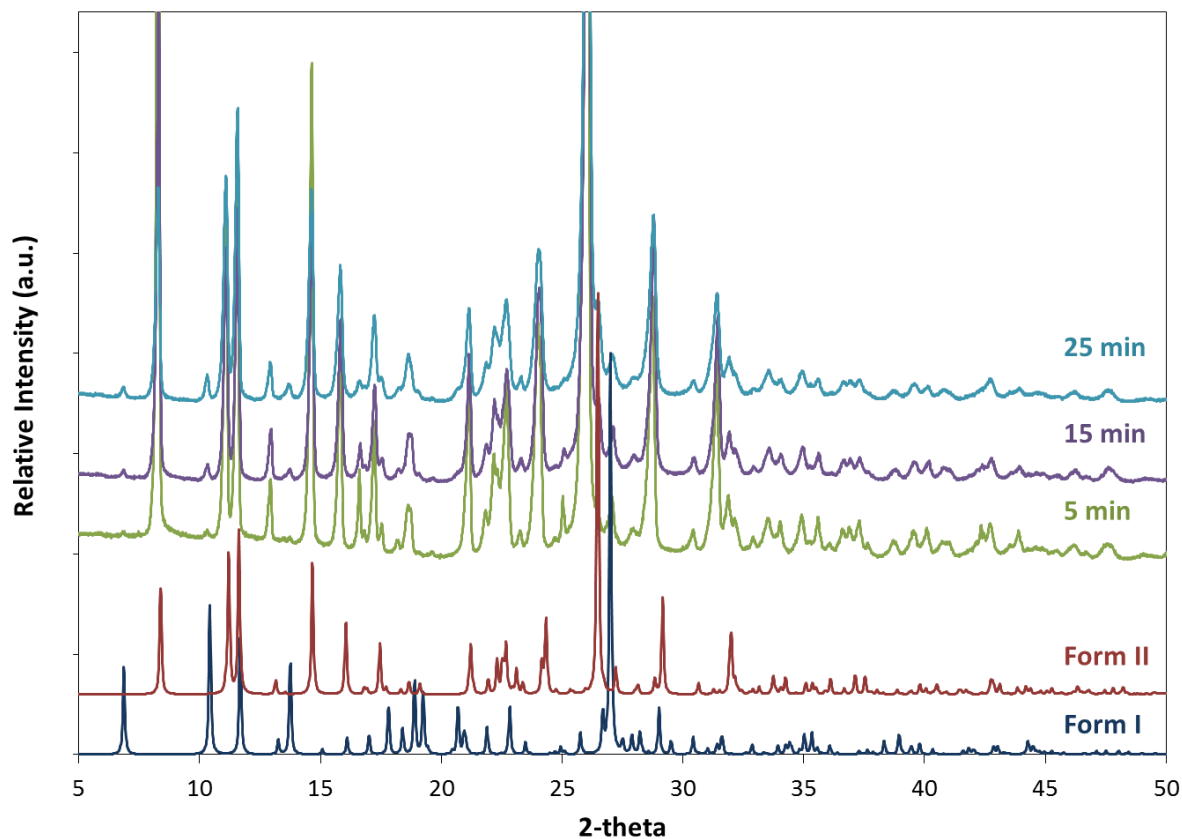
120

121 **Figure 2.** Particle size distribution of unmilled CA-GA cocrystals. $d_{50} = 217 \mu\text{m}$.

122 **Ball Milling**

123 Form II of CA-GA cocrystals were subjected to ball milling for 5, 15 and 25 min. The PXRD
124 patterns of the milled crystals are shown in Figure 3 together with the simulated PXRD patterns
125 for Form I and Form II CA-GA. The signature peaks of Form I at 6.8 and 10.4 2-theta are
126 evident in all the milled samples. This suggests ball milling did not result in any dissociation of
127 the cocrystal into its constituent components as caffeine and glutaric acid but partial
128 transformation from the thermodynamically stable Form II to the metastable Form I occurred
129 even after only 5 min of ball milling. Quantitative analysis of the phase transformation was
130 performed by Rietveld refinements using Topas v4.2 (Bruker-AXS GmbH, Karlsruhe, Germany)

131 following the same procedure as described in our previous report.³⁶ Rietveld refinements show
132 that the amount of Form I increased with ball milling time (Table 1).



133
134 **Figure 3.** PXRD patterns of CA-GA after ball-milled for 5, 15 and 25 minutes.

135

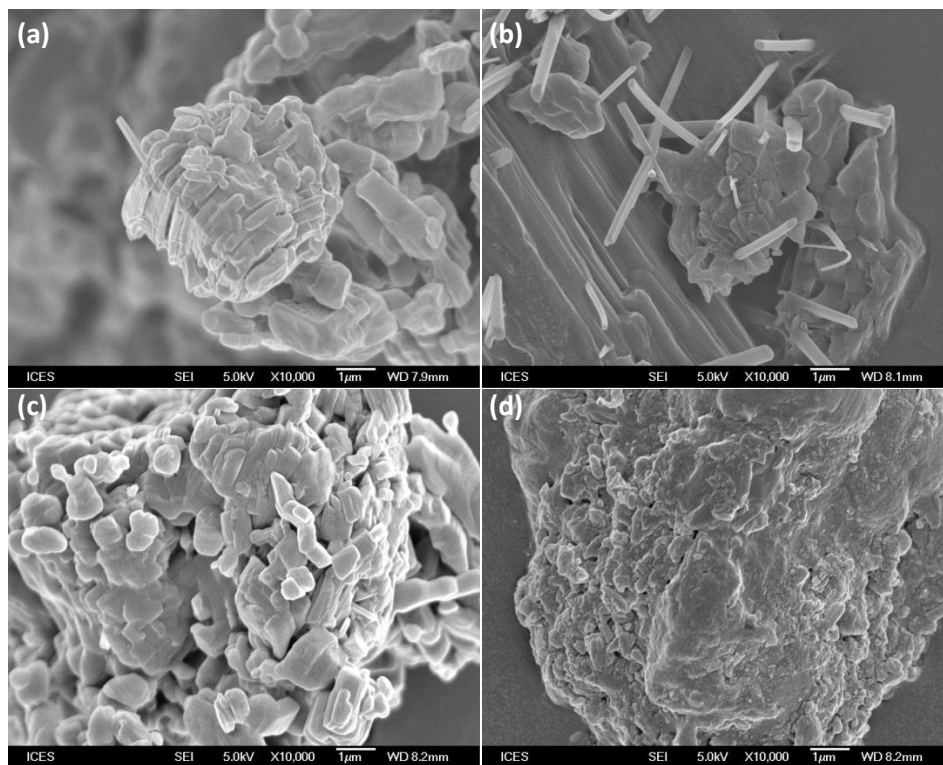
136 **Table 1. Form I content obtained from Rietveld refinements.**

Milling time (min)	Form I (wt %)
5	2.20
15	5.97
25	9.15

137

138

139 The presence of Form I in the milled samples can also be clearly observed from the SEM images
140 (Figure 4). Needle-shaped Form I can be seen amidst the prismatic Form II.



141
142 **Figure 4.** SEM images of CA-GA after ball-milled for (a) 5, (b) 15 and (c,d) 25 minutes.

143 From the d_{50} of the milled samples (Table 2), ball milling was able to reduce the particle size
144 from d_{50} of 217 μm to 69 μm after 5 min of milling. However, increased milling duration did not
145 result in further reduction in d_{50} and instead an increase in d_{50} was observed. The increase in size
146 with milling time is described as “the negative grinding phenomenon”³⁷ which is generally
147 attributed to the aggregation and agglomeration of particles.³⁸ This appeared to be the case in
148 our experiments as larger extent of agglomeration with increase in milling time can be clearly
149 seen from the SEM images in Figure 4. From the PSD (Figure S2, SI), there is a clear shift of

150 particle size toward the coarser fraction and it can be seen that fines below 10 μm have almost all
151 disappeared after 25 min of milling.

152 **Table 2. d_{50} of ball-milled samples measured by Malvern Mastersizer.***

Milling time (min)	d_{50} (μm)	SPAN
0	217	2.185
5	69	2.334
15	72	2.787
25	204	2.658

153 * PSDs are included in Figure S2 in Supplementary Information

154 **Jet Milling**

155 Jet milling was performed on CA-GA Form II at the conditions listed in Table 3. Regardless of
156 the conditions employed, Form II remained intact during jet milling and no Form I was
157 detectable from the PXRD patterns (Figure 5). SEM images (Figure 6) of the jet-milled samples
158 showed no needle-shaped Form I crystals and agglomeration of crystals appeared minimal. More
159 SEM images are included in Figure S3 in the SI. Since the optimization of milling conditions
160 was not the objective of this work, PSD of the jet-milled samples were only measured for three
161 runs to illustrate the particle size reduction after jet milling as shown in Table 3. As expected,
162 intensifying the milling condition by increasing the grinding pressure during jet milling resulted
163 in further reduction of d_{50} from 88 to 29 μm . The width of the PSD (SPAN) also decreased with
164 increasing grinding pressure.

165

166

167

168

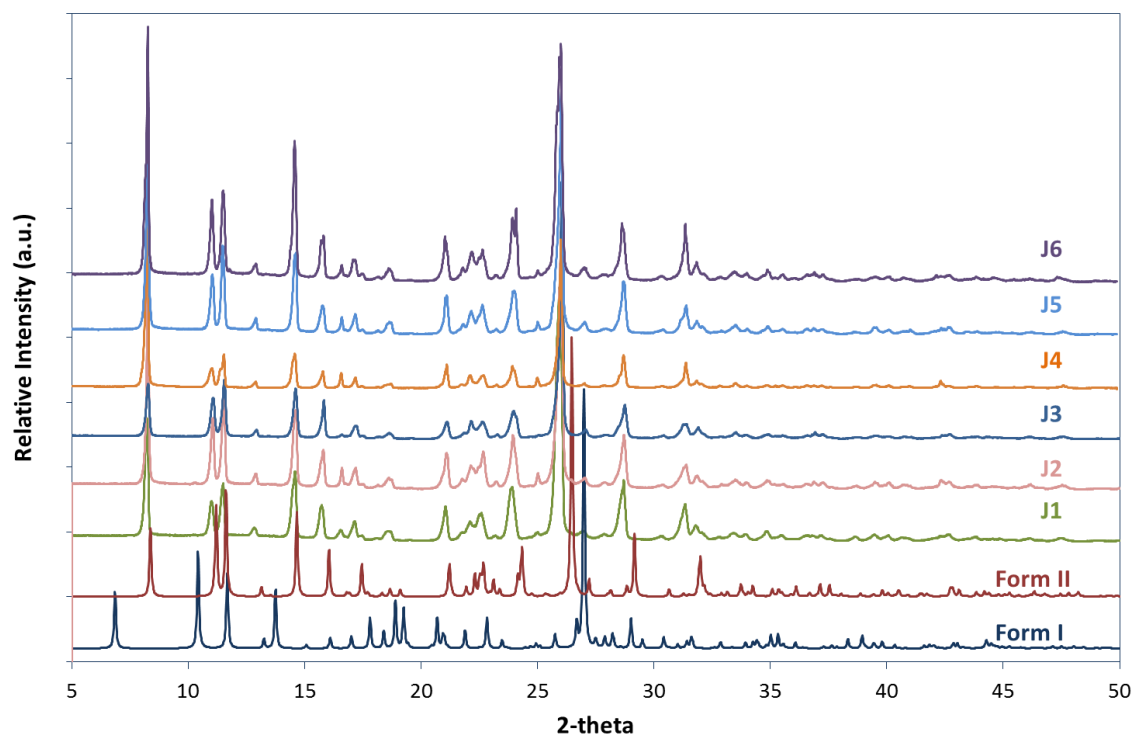
Table 3. Jet milling Conditions and d_{50} Measured by Malvern Mastersizer.*

No.	Injection pressure (bar)	Grinding pressure (bar)	d_{50} (μm)	SPAN
J1	4	1	88	3.430
J2	4	2	29	1.757
J3	4	3	19	1.379
J4	2.5	2	-	-
J5	3.0	2	-	-
J6	3.5	2	-	-

169

* PSDs are included in Figure S4 in supporting information

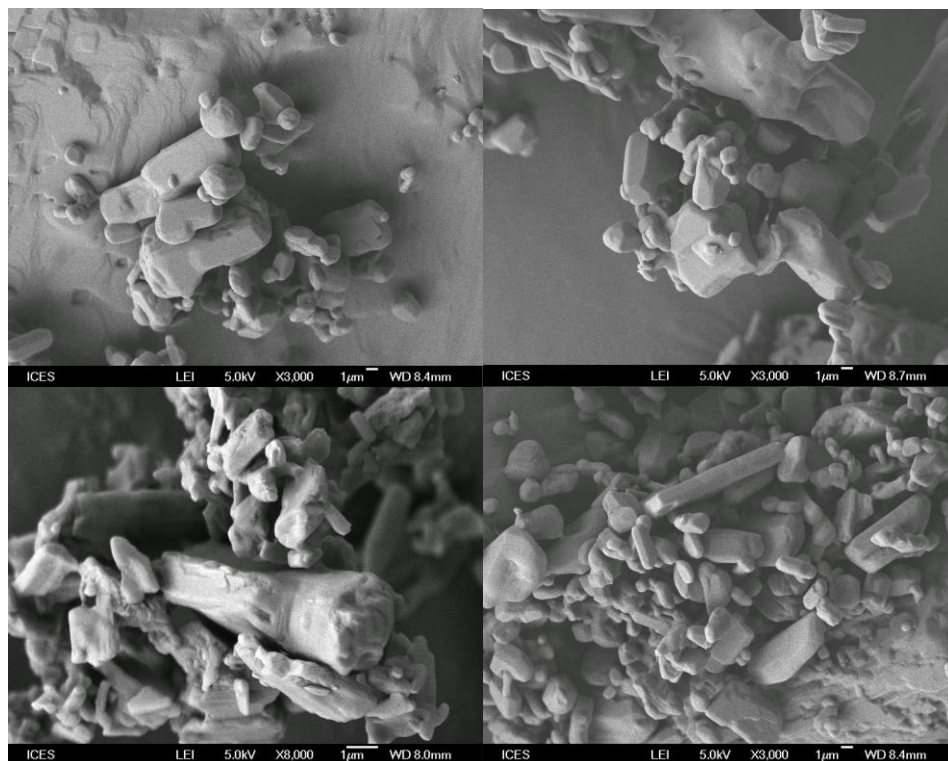
170



171

172 **Figure 5.** PXRD patterns of CA-GA after being jet-milled under different conditions. No Form I

173 could be detected.

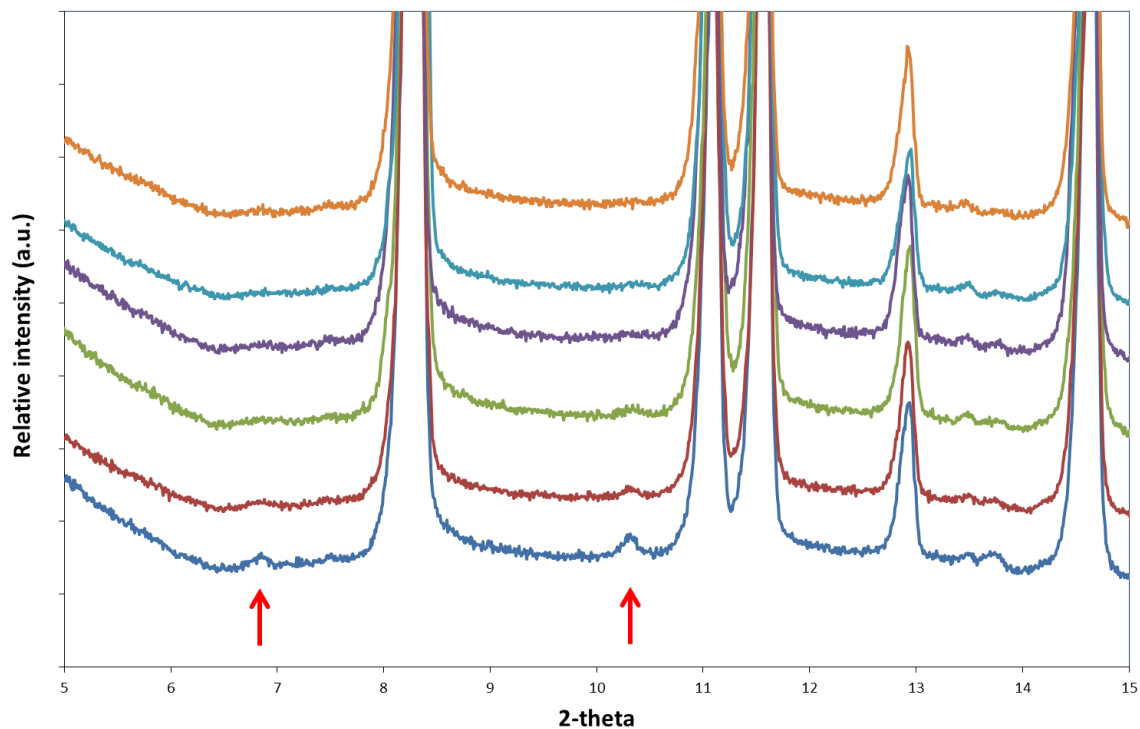


174

175 **Figure 6.** Representative SEM images of jet milled samples.

176 **Post-milling Stability**

177 Milled samples were stored in a desiccator containing P_2O_5 (~ 0% RH) at 22 °C to investigate the
178 post-milling stability. Figure 7 showed the PXRD of CA-GA after ball milling for 5 min. The
179 signature peaks of Form I at 6.8 and 10.4 2-theta can be seen disappearing from day 4 onwards.
180 Trask et al.⁹ have shown that Form I is stable at 0% RH for as long as 7 weeks. The shorter
181 conversion time to Form II observed in our experiment is likely due to the presence of vast
182 excess of Form II that may accelerate the conversion as well as the intermittent exposure to
183 ambient humidity (>70% RH) during sample withdrawal before each PXRD analysis. The
184 reported conversion time is shorter than a day at humidity of 75% RH.⁹



185

186 **Figure 7.** PXRD patterns of ball-milled samples upon storage at 0% RH and room temperature.

187 From bottom: Immediately, 1, 2, 3, 4 and 7 days after ball milling for 5 min. The arrows indicate

188 the signature peaks of Form I.

189

190 All jet milled samples belonged to Form II after milling. Post-milled PXRD analysis showed that

191 the samples remained as Form II, as expected (results not shown).

192 **Comparison between Ball Milling and Jet Milling**

193 Ball milling and jet milling both rely on the particle-particle collision and particle-wall (milling

194 tool) collision to effect size reduction. The mechanisms by which particle size is reduced follow

195 the same principles – existing cracks on the micro- or nanoscale present in the particle are

196 activated when the particle experiences stress and absorb elastic strain energy.³⁹ However, the
197 different modes of operation of these two mill types lead to significant differences to the
198 properties of the milled products. Our experimental findings have shown that jet milling
199 effectively reduced the particle size without incurring any changes to the solid state of the
200 samples. On the other hand, ball milling induced much damage to the samples and size
201 reduction was much less effective than jet milling. Negative-grinding phenomenon was also
202 observed as ball milling duration increased. These observations could be explained by the
203 intensive conditions that the particles experienced during ball milling. During planetary ball
204 milling, the collision process between the particles and between particles and the milling parts
205 (milling balls and wall of the milling jar) over a much longer duration could lead to significant
206 temperature increase inside the milling jar. When particles are subjected to impact and friction
207 forces in the ball mill, mechanical forces result in cracks in the crystals. As the crack propagates
208 at high speed (in the order of 10^2 m/s), crack tip temperature can rise to a temperature much
209 higher than the bulk temperature.⁴⁰ While the temperature surrounding a crack in ductile metals
210 ranges from 450 to 1400 °C,⁴¹ significant heating was also observed for soft polymer material,
211 e.g. 80 °C for PMMA. With such a temperature increase, it is clear that damages to the powder
212 are possible. It has been suggested that during milling, the intense mechanical energy can lead to
213 local heating such that small crystalline regions start to melt.⁴² If the milled material is
214 subsequently quench cooled to below the glass transition temperature (T_g), e.g. in cryomilling,
215 amorphous regions can be obtained from the melt. At temperature higher than T_g , the transiently
216 formed amorphous state will transform to the stable crystal phase.³² Since our experiments were
217 not performed at temperature below T_g , the possibility of amorphous formation can be ruled out.

218 In the case of CA-GA, polymorphic conversion and agglomeration of crystals were observed
219 under the milling conditions used. To understand why such changes were induced, it is
220 necessary to revisit the polymorphism of CA-GA that we have studied previously.³⁶ From the
221 VTXRD results, Form II begins to transform to Form I at around 69 °C. Further heating results
222 in melting at 98 °C. Upon cooling to 78 °C, Form I nucleated and remained to be the only phase
223 observed at the end of the cooling process at 25 °C. As discussed before, the temperature of the
224 powder could easily surpass the transformation temperature of 69 °C during ball milling. This
225 explains why the stable Form II was partially transformed to the metastable Form I. As the
226 milling time increased, the surface of some of the crystals may increase to beyond the melting
227 point of Form I, i.e. 98 °C, in which case small amount of crystals surface may melt giving rise
228 to melted regions on the crystal surface. As the crystals continue to collide with each other, the
229 tiny melt regions on the crystal surface start to coalesce to form liquid bridges between the
230 crystals. The liquid bridges then recrystallize to Form I upon cooling to below 78 °C by the
231 dissipation of energy through contact with air inside the milling jar. Once recrystallized, Form I
232 remains till the end of the experiment. The formation and solidification of liquid bridges could
233 explain the observed agglomeration and appearance of Form I at longer milling time. This
234 melting of the crystal surface is evident in Figure 4d as the crystal edges look fused, in contrast
235 to the sharp edge of crystals obtained from jet milling (Figure 6). In summary, we propose two
236 different mechanisms for the observations in ball milling experiments. At short milling time, the
237 local temperature of the crystals increased to above the polymorphic transformation of 69 °C,
238 leading to the partial transformation of stable Form II to metastable Form I. At longer milling
239 time, the local temperature of the crystals increased to above the melting point of Form I at 98
240 °C. Surface melting occurred, giving rise to tiny melt regions on the crystal surface which then

241 coalesce to form liquid bridges between crystals upon collision between crystals. The liquid
242 bridges then solidified and recrystallization of Form I took place, resulting in the appearance of
243 Form I and crystals agglomeration. Therefore, at longer milling time, increase in d_{50} and width
244 of distribution were observed.

245 In a typical jet mill, powders are fed into the grinding chamber via a vibrating feeder that
246 controls the feed rate. The powders are accelerated to a high velocity by an air jet prior to
247 entering the grinding chamber. The pressure of the feeding stream is called the injection
248 pressure. Another air jet enters the grinding chamber through specifically designed and spatially
249 orientated grinding nozzles which accelerate the powder to supersonic speeds and create extreme
250 turbulence inside the grinding chamber. The turbulence and orbital nature of the grinding
251 chamber facilitates multiple particle-particle and particle-wall collisions at a higher frequency
252 and induces particle fracture and size reduction. Unlike ball milling, no heating effect is
253 generated during jet milling.⁴³ This is because of the countering cooling arising from the Joule-
254 Thompson effect when compressed gas rapidly expands to atmospheric pressure when passing
255 through the grinding nozzle. Therefore, jet milling is often the method of choice for heat
256 sensitive material. This also explains why jet milling was effective in reducing the particle size
257 of CA-GA without inducing any change to the solid state of the crystals. Moreover, owing to the
258 design of the spiral jet mill, size reduction and classification are accomplished simultaneously.
259 Within the grinding chamber, two dominant forces are acting on the particles: the inertia
260 centrifugal force and the fluid drag force. The fluid drag force is caused by the gas flow towards
261 the exit at the center of the mill. If the drag force is larger than the centrifugal force, the particle
262 will exit the mill; otherwise, it will stay in the grinding chamber and continue to fracture until it
263 is small enough to exit the chamber. The cut size, size at which the particle exits the mill, can be

264 controlled by the operating parameters such as feed rate and grinding pressure. Therefore, in our
265 case, the particle size of CA-GA could be continually reduced by intensifying the milling
266 conditions, e.g. increasing grinding pressure (Table 3).

267 **Practical Implications**

268 In this work, jet milling was found to be an effective and suitable micronization method for CA-
269 GA cocrystal. Ball milling, on the other hand, was not effective in reducing particle size and
270 much damage was incurred on the samples in terms of both polymorphic purity and
271 agglomeration. For pharmaceutical compounds, the thermal effects of ball milling could be a
272 major issue since the API generally has a polymorphic transformation temperature and melting
273 point within the range of possible temperature rise during ball milling as discussed earlier on.
274 CA-GA polymorphic transformation during ball milling can be explained by the thermal effect
275 experienced by the material. However, the effect of ball milling on other chemicals can be more
276 complicated and unpredictable. Hedoux et al.²⁸ found that ball milling induced transformation of
277 each form of anhydrous caffeine toward the other, and given long enough grinding, an
278 equilibrium state composed 30% of Form II was attained. Detailed explanation of the observed
279 phenomenon was not given but the authors proposed that it was probably related to the nature of
280 the disorder-disorder transformation and stability conditions of caffeine Form I at room
281 temperature. Therefore, care should be exercised in ball milling of co-crystals for the purpose of
282 particle size reduction at the final stage of pharmaceuticals manufacturing. Nevertheless, ball
283 milling is a valuable tool for small-scale solid-form screening as demonstrated by Jones and
284 coworkers³⁵ as well as chemical synthesis by mechanochemical reactions.⁴⁴⁻⁴⁷

285 Given the potential stability problem associated with the exposure to water or solvent, it can be
286 foreseen that unit operations utilizing water or solvent such as wet milling and granulation could
287 problematic for cocrystal and perhaps best avoided unless the phase diagram of the cocrystal
288 with the said solvent is thoroughly investigated to identify the safe region of operation, if any.
289 This is especially important for cocrystals of hydrate forming compound as such as CA-GA. In
290 addition to polymorphic transformation when subject to mechanical stress and heating, these
291 cocrystals may undergo dissociation and subsequent hydrate recrystallization on exposure to
292 water. Eddeleston et al.⁴⁸ demonstrated that even exposure to high humidity condition is
293 sufficient to induce significant levels of cocrystal dissociation for caffeine cocrystals. During wet
294 granulation, the combination of granulating solvent and drying conditions also provide a suitable
295 environment for polymorphic conversion and solvate formation. Crystal form conversion during
296 wet granulation has been reported for several pharmaceutical compounds but such study has yet
297 to be performed on cocrystal system.

298

299 ▪ **CONCLUSIONS**

300 The results from this investigation show that jet milling is a more suitable size reduction
301 method than ball milling for caffeine-glutaric cocrystals. Ball milling induced polymorphic
302 transformation of CA-GA from the stable Form II to the metastable Form I and the particle size
303 was not reduced but increased with increasing milling time. On the other hand, jet milling did
304 not alter the solid state integrity of CA-GA and the particle size was reduced effectively. The
305 difference in the performance of the two mill types was explained by the heating effect during
306 ball milling. Depending on the ball milling time, we propose that the local temperature of

307 crystals could increase to above the polymorphic transformation temperature of 69 °C or even the
308 melting point of Form I at 98 °C, leading to partial transformation of stable Form II to metastable
309 Form I or even surface melting and subsequent recrystallization of Form I from melt. The
310 plausible formation of liquid bridges between crystals and subsequent recrystallization also result
311 in crystals agglomeration and thus explains the “negative” grinding phenomenon observed with
312 increasing ball milling time. Due to the Joule-Thomson effect, the cocrystals did not experience
313 any net heating during jet milling and thus the solid-state integrity of the cocrystals was
314 preserved. The findings from this study have broader implication to the selection of mill type
315 for not only pharmaceutical cocrystal but pharmaceutical compounds in general.

316

317 ▪ **ASSOCIATED CONTENT**

318 **Supporting Information.** It contains figures of Differential Scanning Calorimetry of CA-GA
319 (Form II) cocrystal, Particle Size Distributions (PSDs) of ball-milled samples, Scanning Electron
320 Microscopy images of jet-milled samples and PSDs of jet-milled samples. This information is
321 available free of charge via the Internet at <http://pubs.acs.org/>.

322

323 ▪ **AUTHOR INFORMATION**

324 **Corresponding Author**

325 *E-mail: ann_chow@ices.a-star.edu.sg. Tel: (65) 6796 3843; Fax: 65 6316 6183.

326 ▪ **ACKNOWLEDGEMENT**

327 This work was supported by Science and Engineering Research Council of A*STAR
328 (Agency for Science, Technology and Research), Singapore. We thank Dr Zaiqun Yu for
329 providing the caffeine-glutaric acid 1:1 cocrystals and Dr Martin Schreyer for performing the
330 Rietveld refinements.

331

332 ■ REFERENCES

333 (1) Aitipamula, S.; Vangala, V. R.; Chow, P. S.; Tan, R. B. H., A cocrystal hydrate of an
334 antifungal agent, griseofulvin, with improved physicochemical properties. *Cryst. Growth Des.*
335 **2012**, *12*, 5858-5863.

336 (2) Almarsson, O.; Zaworotko, M. J., Crystal engineering of the composition of
337 pharmaceutical phases. Do pharmaceutical co-crystals represent a new path to improved
338 medicines? *Chem. Commun.* **2004**, 1889-1896.

339 (3) Bak, A.; Gore, A.; Yanez, E.; Stanton, M.; Tufekcic, S.; Syed, R.; Akrami, A.; Rose, M.;
340 Surapaneni, S.; Bostick, T.; King, A.; Neervannan, S.; Ostovic, D.; Koparkar, A., The co-crystal
341 approach to improve the exposure of a water-insoluble compound: AMG 517 sorbic acid co-
342 crystal characterization and pharmacokinetics. *J. Pharm. Sci.* **2008**, *97*, 3942-3956.

343 (4) Basavoju, S.; Bostrom, D.; Velaga, S. P., Pharmaceutical cocrystal and salts of
344 norfloxacin. *Cryst. Growth Des.* **2006**, *6*, 2699-2708.

345 (5) Good, D. J.; Rodriguez-Hornedo, N., Solubility advantage of pharmaceutical cocrystals.
346 *Cryst. Growth Des.* **2009**, *9*, 2252-2264.

347 (6) Jones, W.; Motherwell, S.; Trask, A. V., Pharmaceutical cocrystals: An emerging
348 approach to physical property enhancement. *MRS Bull.* **2006**, *31*, 875-879.

349 (7) Schultheiss, N.; Newman, A., Pharmaceutical cocrystals and their physicochemical
350 properties. *Cryst. Growth Des.* **2009**, *9*, 2950-2967.

351 (8) Stanton, M. K.; Kelly, R. C.; Colletti, A.; Kiang, Y.-H.; Langley, M.; Munson, E. J.;
352 Peterson, M. L.; Roberts, J.; Wells, M., Improved pharmacokinetics of AMG 517 through co-
353 crystallization part 1: Comparison of two acids with corresponding amide co-crystals. *J. Pharm.*
354 *Sci.* **2010**, *99*, 3769-3778.

355 (9) Trask, A. V.; Motherwell, W. D. S.; Jones, W., Pharmaceutical cocrystallization:
356 Engineering a remedy for caffeine hydration. *Cryst. Growth Des.* **2005**, *5*, 1013-1021.

357 (10) Trask, A. V.; Motherwell, W. D. S.; Jones, W., Physical stability enhancement of
358 theophylline via cocrystallization. *Int. J. Pharm.* **2006**, *320*, 114-123.

359 (11) Vangala, V. R.; Chow, P. S.; Tan, R. B. H., Characterization, physicochemical and
360 photo-stability of co-crystal involving an antibiotic drug, nitrofurantoin, and 4-hydroxybenzoic
361 acid. *CrystEngComm* **2011**, *13*, 759-762.

- 362 (12) Trask, A. V., An overview of pharmaceutical cocrystals as intellectual property. *Mol.*
363 *Pharm.* **2007**, *4*, 301-309.
- 364 (13) Vishweshwar, P.; McMahon, J. A.; Peterson, M. L.; Hickey, M. B.; Shattock, T. R.;
365 Zaworotko, M. J., Crystal engineering of pharmaceutical co-crystals from polymorphic active
366 pharmaceutical ingredients. *Chem. Commun.* **2005**, 4601-4603.
- 367 (14) Halebian, J.; McCrone, W., Pharmaceutical applications of polymorphism. *J. Pharm.*
368 *Sci.* **1969**, *58*, 911-929.
- 369 (15) McCrone, W. C., *Polymorphism in Physics and Chemistry of the Solid State*. ed.;
370 Interscience: New York, 1965; Vol. 2, p 725-767.
- 371 (16) Bolla, G.; Mittapalli, S.; Nangia, A., Celecoxib cocrystal polymorphs with cyclic amides:
372 synthons of a sulfonamide drug with carboxamide coformers. *CrystEngComm* **2014**, *16*, 24-27.
- 373 (17) Aitipamula, S.; Chow, P. S.; Tan, R. B. H., Polymorphism in cocrystals: a review and
374 assessment of its significance. *CrystEngComm* **2014**, *16*, 3451-3465.
- 375 (18) Chun, N.-H.; Wang, I.-C.; Lee, M.-J.; Jung, Y.-T.; Lee, S.; Kim, W.-S.; Choi, G. J.,
376 Characteristics of indomethacin–saccharin (IMC–SAC) co-crystals prepared by an anti-solvent
377 crystallization process. *Eur. J. Pharm. Biopharm.* **2013**, *85*, 854-861.
- 378 (19) Sheikh, A. Y.; Rahim, S. A.; Hammond, R. B.; Roberts, K. J., Scalable solution
379 cocrystallization: Case of carbamazepine-nicotinamide I. *Crystengcomm* **2009**, *11*, 501-509.
- 380 (20) Yu, Z. Q.; Chow, P. S.; Tan, R. B. H., Operating regions in cooling cocrystallisation of
381 caffeine and glutaric acid in acetonitrile. *Cryst. Growth Des.* **2010**, *10*, 2382-2387.
- 382 (21) Yu, Z. Q.; Chow, P. S.; Tan, R. B. H.; Ang, W. H., Supersaturation control in cooling
383 polymorphic co-crystallization of caffeine and glutaric Acid. *Cryst. Growth Des.* **2011**, *11*,
384 4525–4532.
- 385 (22) Yu, Z. Q.; Chow, P. S.; Tan, R. B. H.; Ang, W. H., PAT-enabled determination of design
386 space for seeded cooling crystallization. *Org. Process Res. Dev.* **2013**, *17*, 549-556.
- 387 (23) Zhang, G. G. Z.; Law, D.; Schmitt, E. A.; Qiu, Y., Phase transformation considerations
388 during process development and manufacture of solid oral dosage forms. *Adv. Drug Deliver.*
389 *Rev.* **2004**, *56*, 371-390.
- 390 (24) Newman, A.; Zografi, G., Critical considerations for the qualitative and quantitative
391 determination of process-induced disorder in crystalline solids. *J. Pharm. Sci.* **2014**, *103*, 2595-
392 2604.
- 393 (25) Chieng, N.; Zujovic, Z.; Bowmaker, G.; Rades, T.; Saville, D., Effect of milling
394 conditions on the solid-state conversion of ranitidine hydrochloride form I. *Int. J. Pharm.* **2006**,
395 *327*, 36-44.
- 396 (26) de Gusseme, A.; Neves, C.; Willart, J. F.; Rameau, A.; Descamps, M., Ordering and
397 disordering of molecular solids upon mechanical milling: the case of Fanserine. *J. Pharm. Sci.*
398 **2008**, *97*, 5000-5012.
- 399 (27) Descamps, M.; Willart, J. F.; Dudognon, E.; Caron, V., Transformation of
400 pharmaceutical compounds upon milling and comilling: the role of Tg. *J. Pharm. Sci.* **2007**, *96*,
401 1398-1407.
- 402 (28) Hédoux, A.; Guinet, Y.; Paccou, L.; Danède, F.; Derollez, P., Polymorphic
403 transformation of anhydrous caffeine upon grinding and hydrostatic pressurizing analyzed by
404 low-frequency Raman spectroscopy. *J. Pharm. Sci.* **2013**, *102*, 162-170.

- 405 (29) Hu, Y.; Erxleben, A.; Hodnett, B. K.; Li, B.; McArdle, P.; Rasmuson, Å. C., Solid-state
406 transformations of sulfathiazole polymorphs: the effects of milling and humidity. *Cryst. Growth*
407 *Des.* **2013**, *13*, 3404-3413.
- 408 (30) Linol, J.; Coquerel, G., Influence of high energy milling on the kinetics of the
409 polymorphic transition from the monoclinic form to the orthorhombic form of (±)5-methyl-5-(4'-
410 methyl-phenyl)hydantoin. *J. Therm. Anal. Calorim.* **2007**, *90*, 367-370.
- 411 (31) Németh, Z.; Sztatisz, J.; Demeter, A., Polymorph transitions of bicalutamide: a remarkable
412 example of mechanical activation. *J. Pharm. Sci.* **2008**, *97*, 3222-3232.
- 413 (32) Trasi, N. S.; Boerrigter, S. X. M.; Byrn, S. R., Investigation of the milling-induced
414 thermal behavior of crystalline and amorphous griseofulvin. *Pharm. Res.* **2010**, *27*, 1377-1389.
- 415 (33) Boldyreva, E. Mechanochemistry of inorganic and organic systems: what is similar, what
416 is different? *Chem. Soc. Rev.* **2013**, *42*, 7719-7738.
- 417 (34) Griesser, U. J.; Burger, A., The effect of water vapor pressure on desolvation kinetics of
418 caffeine 4/5-hydrate. *Int. J. Pharm.* **1995**, *120*, 83-93.
- 419 (35) Trask, A. V.; Motherwell, W. D. S.; Jones, W., Solvent-drop grinding: green polymorph
420 control of cocrystallisation. *Chem. Commun.* **2004**, 890-891.
- 421 (36) Vangala, V. R.; Chow, P. S.; Schreyer, M.; Lau, G.; Tan, R. B. H., Thermal and in Situ
422 X-ray diffraction analysis of a dimorphic co-crystal, 1:1 caffeine–glutaric Acid. *Cryst. Growth*
423 *Des.* **2016**, *16*, 578-586.
- 424 (37) Jimbo, G.; Zhao, Q. Q.; Yokoyana, T.; Taniyana, Y. In *The grinding limit and the*
425 *negative grinding phenomenon*, 2nd World Congress Particle Technology, Kyoto, Japan, 1990,
426 1990; Funtai, K. g., Ed. Society of Powder Technology in association with VDI-Gesellschaft
427 Verfahrenstechnik, Fine Particle Society: Kyoto, Japan, 1990; pp 305-312.
- 428 (38) Baláž, P., High-energy milling. In *Mechanochemistry in Nanoscience and Minerals*
429 *Engineering*, Springer: Berlin Heidelberg, 2008; p 122.
- 430 (39) Saleen, I. Y.; Smyth, H. D. C., Micronization of a soft materials: air-jet and micro-ball
431 milling. *AAPS PharmSciTech* **2010**, *11*, 1642-1649.
- 432 (40) Weichert, R., Anwendung von Fehlstellenstatistik und Bruchmechanik zur Beschreibung
433 von Zerkleinerungsvorgaengen. *Zement-Kalk-Gips* **1992**, *45*, 1-8.
- 434 (41) Zehnder, A. T.; Rosakis, A. J., On the temperature distribution at the vicinity of
435 dynamically propagating cracks in 4340 steel. *J. Mech. Phys. Solids* **1991**, *39*, 385-415.
- 436 (42) Feng, T.; Pinal, R.; Carvajal, M. T., Process induced disorder in crystalline materials:
437 differentiating defective crystals from the amorphoous form of Griseofulvin. *J. Pharm. Sci.*
438 **2008**, *97*, 3207-3221.
- 439 (43) Trost, C., Jet mill grinding. *Science* **1953**, *117*, 3-3.
- 440 (44) McKissic, K. S.; Caruso, J. T.; Blair, R. G.; Mack, J., Comparison of shaking versus
441 baking: further understanding the energetics of a mechanochemical reaction. *Green Chem.* **2014**,
442 *16*, 1628-1632.
- 443 (45) Fischer, F.; Wenzel, K.-J.; Rademann, K.; Emmerling, F., Quantitative determination of
444 activation energies in mechanochemical reactions. *Phys. Chem. Chem. Phys.* **2016**, *18*, 23320-
445 23325.
- 446 (46) Uzarevic, K.; Strukil, V.; Mottillo, C.; Julien, P. A.; Puskaric, A.; Friscic, T.; Halasz, I.,
447 Exploring the effect of temperature on a mechanochemical reaction by in situ synchrotron
448 powder X-ray diffraction. *Cryst. Growth Des.* **2016**, *16*, 2342-2347.

449 (47) Tan, D.; Loots, L.; Friscic, T., Towards medicinal mechanochemistry: evolution of
450 milling from pharmaceutical solid form screening to the synthesis of active pharmaceutical
451 ingredients (APIs). *Chem. Commun.* **2016**, 7760.

452 (48) Eddleston, M. D.; Thakuria, R.; Aldous, B. J.; Jones, W., An investigation of the causes
453 of cocrystal dissociation at high humidity. *J. Pharm. Sci.* **2014**, *103*, 2859-2864.

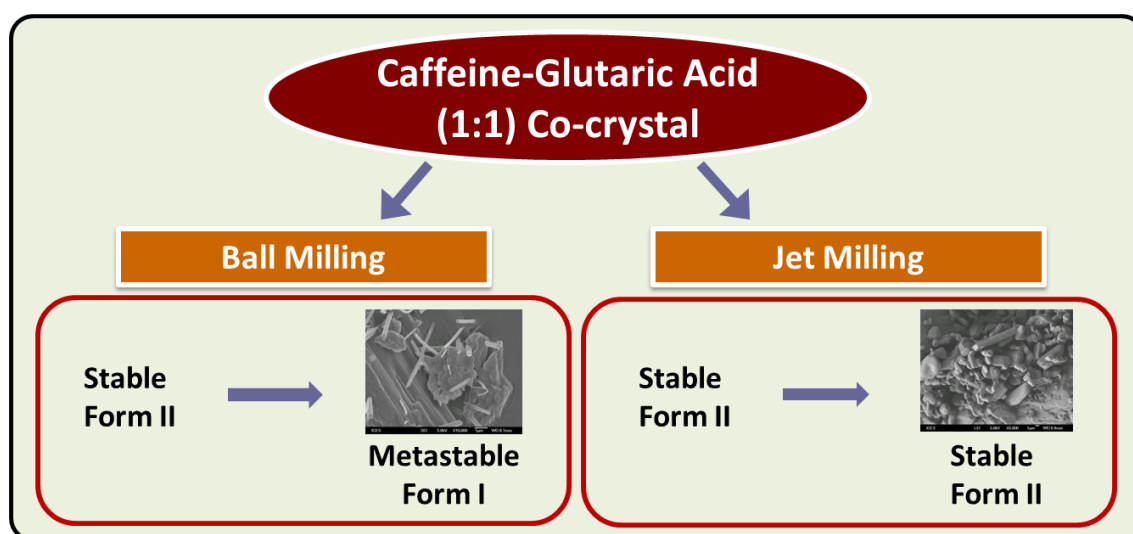
454

455

456

458 **Stability of Pharmaceutical Cocrystal During**
 459 **Milling: A Case Study of 1:1 Caffeine-Glutaric Acid**

460 *Pui Shan Chow,^{*†} Grace Lau,[†] Wai Kiong Ng,[†] and Venu R. Vangala^{†,‡}*



461

462

463 Despite the rising interest in pharmaceutical cocrystals, there is a lack of research in the solid
 464 processing of cocrystals downstream to crystallization. The purpose of this study is to investigate
 465 the effect of milling on dimorphic caffeine-glutaric acid cocrystal using ball/ jet mill. It reveals
 466 that ball milling induced polymorphic transformation from stable Form II to metastable Form I;
 467 whereas Form II remained intact after jet milling. Aside, jet mill was found to be effective in
 468 reducing particle size than ball mill. The difference in the performance of the two types of mill

469 was attributed to the localized heating effect during ball milling and Joule-Thompson countering
470 cooling effect during jet milling.

471

472

473

Supporting Information (SI)

Stability of Pharmaceutical Cocrystal During Milling: A Case Study of 1:1 Caffeine-Glutaric Acid

Pui Shan Chow,^{†} Grace Lau,[†] Wai Kiong Ng,[†] and Venu R. Vangala^{†,‡}*

¶

[†]Crystallisation and Particle Science

Institute of Chemical and Engineering Sciences

A*STAR (Agency for Science, Technology and Research)

1, Pesek Road, Jurong Island, Singapore, 627833.

[‡]Current Affiliation:

Centre for Pharmaceutical Engineering Science

School of Pharmacy, University of Bradford

Bradford BD7 1DP, United Kingdom

Figure S1. DSC thermogram of unmilled CA-GA cocrystal. The data is consistent with the thermal behavior of CA-GA cocrystal reported before.³⁵

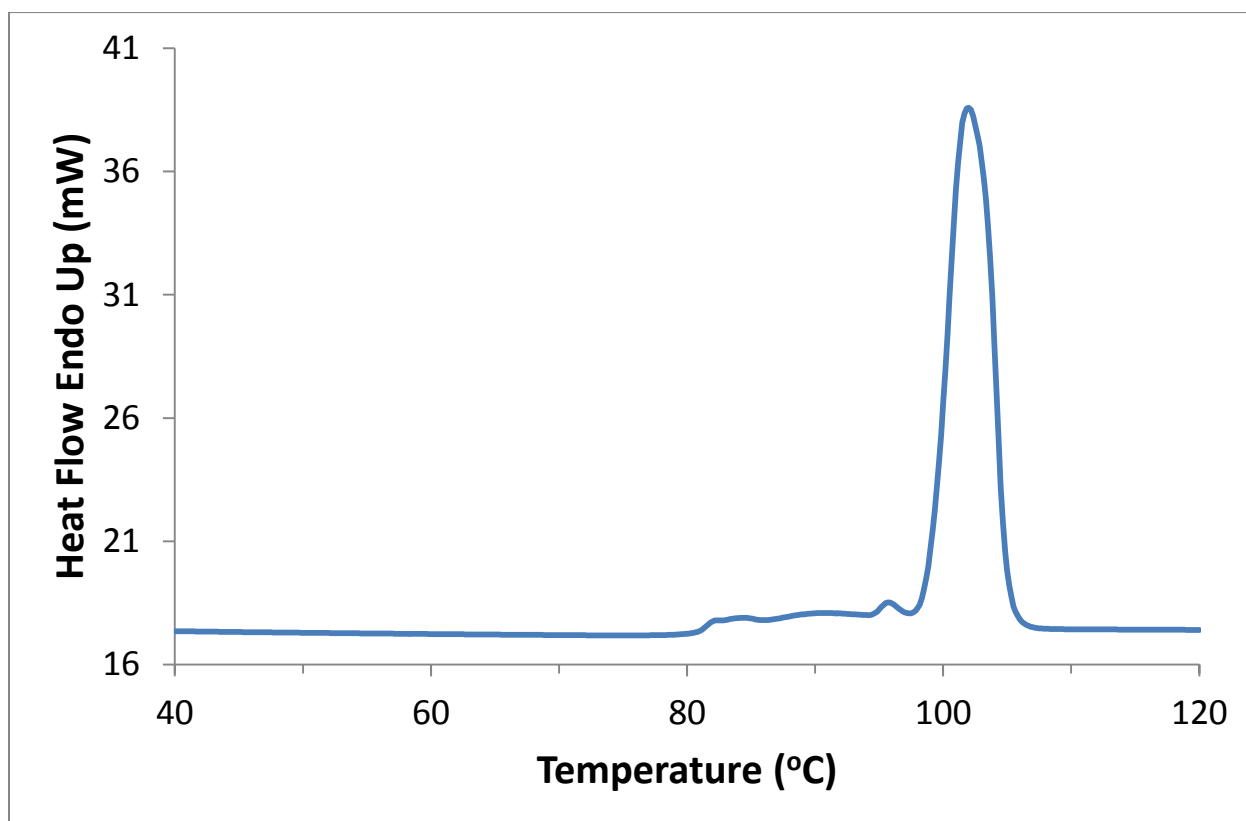
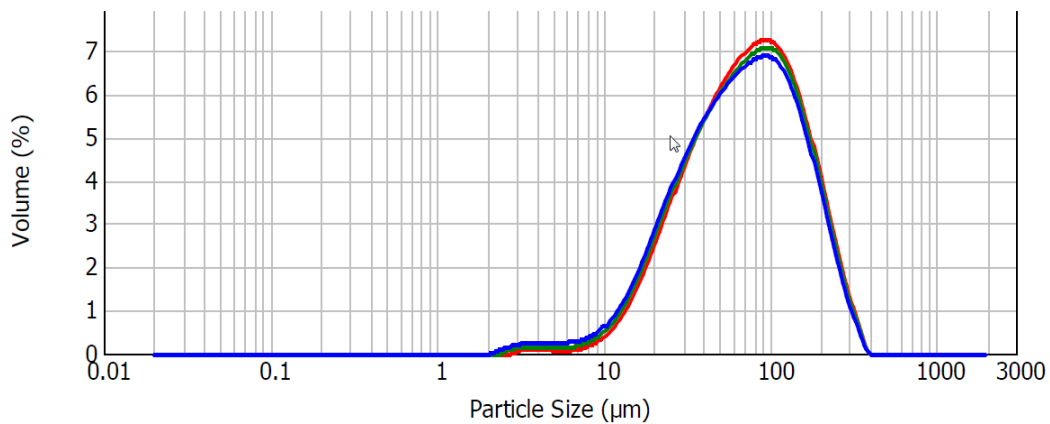
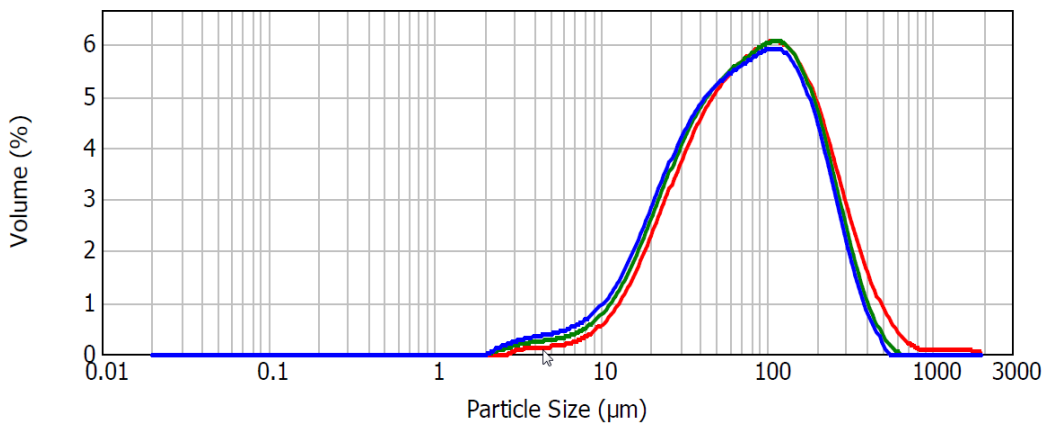


Figure S2. PSDs of ball-milled samples.

(a) 5 min



(b) 15 min



(c) 25 min

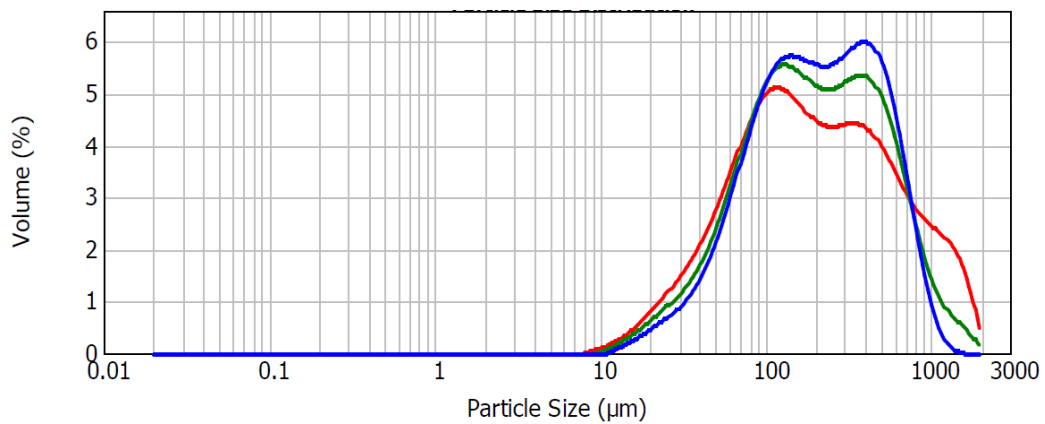
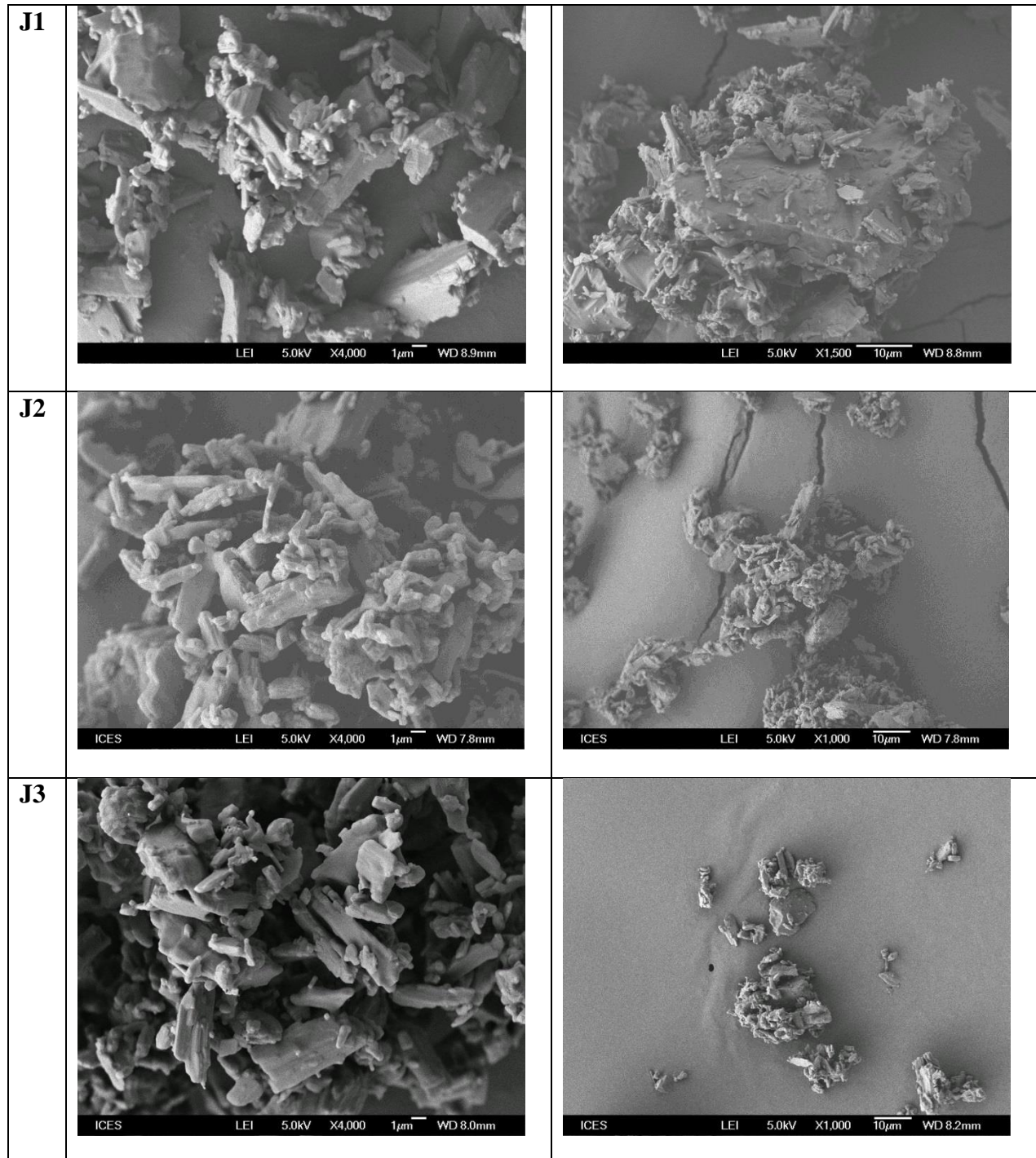
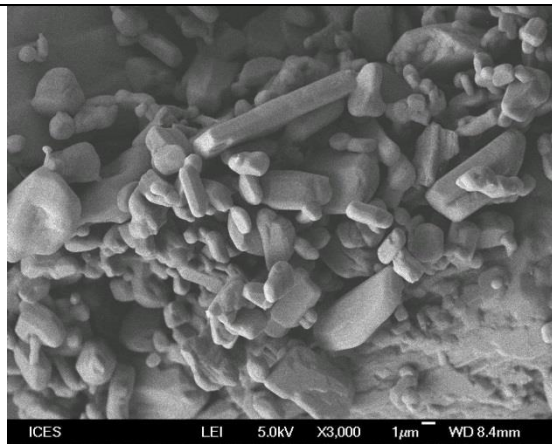
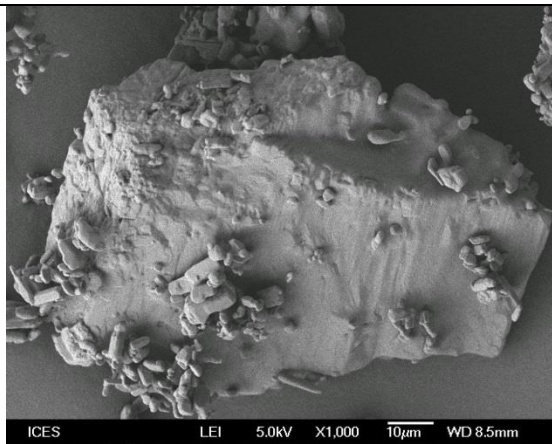


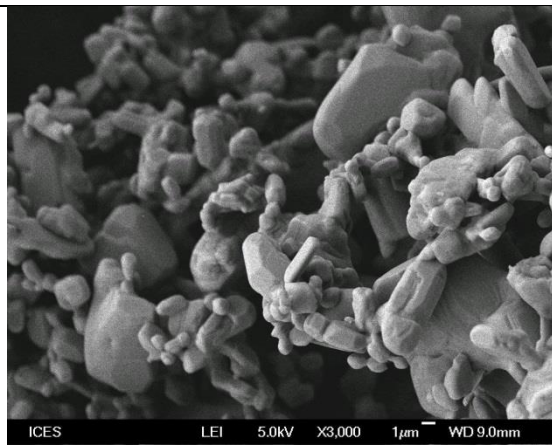
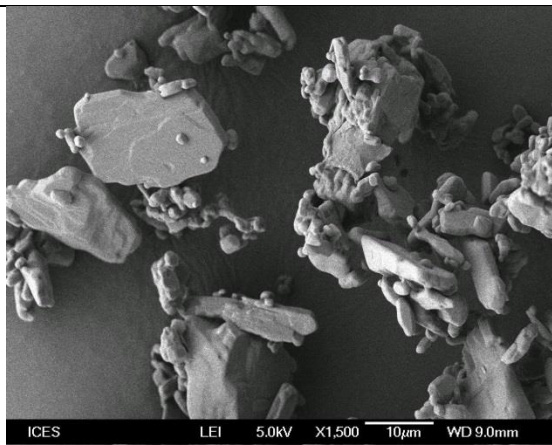
Figure S3. SEM images of jet milled samples.



J4



J5



J6

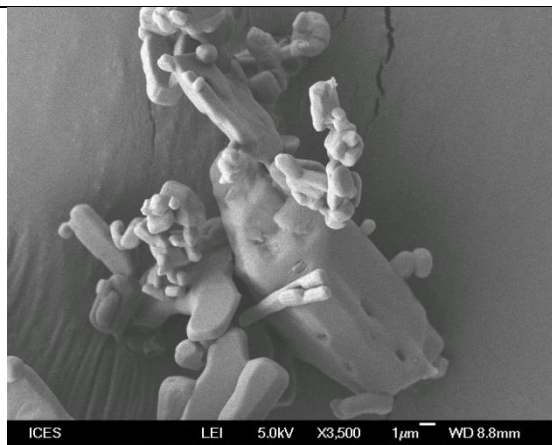
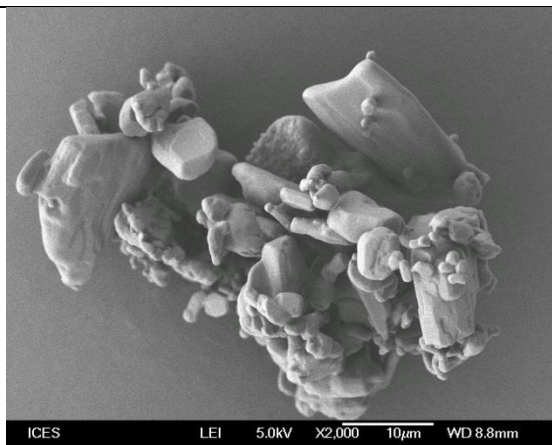


Figure S4. PSDs of jet-milled samples.

